ADVANCED ENERGY MATERIALS

Supporting Information

for *Adv. Energy Mater.*, DOI: 10.1002/aenm.201500968

High Throughput Discovery of Solar Fuels Photoanodes in the $CuO–V_2O_5$ System

Lan Zhou, Qimin Yan, Aniketa Shinde, Dan Guevarra, Paul F. Newhouse, Natalie Becerra-Stasiewicz, Shawn M. Chatman, Joel A. Haber, Jeffrey B. Neaton, and John M. Gregoire**

Supporting Information

High Throughput Discovery of Solar Fuels Photoanodes in the CuO-V_2O_5 System

Lan Zhou, Qimin Yan, Aniketa Shinde, Dan Guevarra, Paul F. Newhouse, Natalie Becerra-Stasiewicz, Shawn M. Chatman, Joel A. Haber, Jeffrey B. Neaton, John M. Gregoire[*]*

1. Literature notes on polymorphs of copper orthovanadate

Table S1: Literature of polymorphs and phase transitions in copper orthovanadate ($Cu_3V_2O_8$)

Mineral Name			**Reference**	**ICSD**	**Label**	**Materials Project id**
McBirneyite	triclinic	P-1	Hughes 1987[1]	00-044-1480		504747
Pseudolyonsite	monoclinic	$P2_1/c$	Zelenski 2011[2]	01-074-1503		600273
Synthetic	monoclinic	$P2_1/c$	Shannon 1972[3]	01-074-1503	β-phase[#]	
			Rogado 2003[4]			
			Min 2011[5]			
			Zhang 2013[6]			
			Seabold 2015[7]			
	triclinic	P-1	Brisi 1958[8]	00-016-0419[*]	α-phase[+]	
	unknown		Coing-Boyat 1982[9]	01-074-1401	γ-phase[?]	
Transitions						
α,β,γ transition			Rao 1993[10]			
α to β			Rogado 2003[4]			
monoclinic to triclinic			Min 2011[5]		β to γ [?]	

[*] 00-016-0419 is replaced by 00-044-1480

[+] α-phase is referred to by Rogado 2003, it seems to match Rao 1993 α-phase

[#] β-phase is referred to by Rogado 2003

[?] phase assignments are questionable

McBirneyite (Hughes 1987) and Pseudolyonsite (Zelenski 2011) are two natural mineral species of $Cu_3V_2O_8$. McBirneyite is triclinic with space group P-1, while Pseudolyonsite is monoclinic, $P2_1/c$.

The first synthetic McBirneyite phase $Cu_3V_2O_8$ (ICSD card 00-016-0419, replaced by 00-044-1480, which was obtained by Hughes 1987 on natural McBirneyite mineral), one of the equilibrium phases in CuO-V_2O_5 phase diagram, was obtained by the conventional solid state reaction technique (Brisi and Molinari 1958). Rogado 2003 claimed that this phase is called α- $Cu_3V_2O_8$. Later Coing-Boyat (1982) obtained 1747 powder diffraction peaks on their $Cu_3V_2O_8$ phase (ICSD card 01-074-1401), and the strongest peaks are observed in our PVD $Cu_3V_2O_8$ phase (McBirneyite).

Shannon 1972 synthesized monoclinc $Cu_3V_2O_8$ phase, which later is called β-phase by Rogado 2003, (ICSD card 01-074-1503). This monoclinic β-$Cu_3V_2O_8$ (space group: $P2_1/c$) can be obtained by (1) heating triclinic $Cu_3V_2O_8$ (Brisi 1958 phase) at a temperature of 900°C and at high pressure (30, 40 kbar)

(Shannon 1972, Rogado 2003); (2) through the calcination of precursor $Cu_3V_2O_7(OH)_2{\cdot}2H_2O$ at 500°C for hours (Min 2011, Zhang 2013); (3) dip coating precursor $Cu_3V_2O_7(OH)_2{\cdot}2H_2O$ onto FTO coated glass and dried on a hot plate preheated to 300°C for 2 min, then annealed in a tube furnace open to ambient air at 425°C for 1 h, preceded by a 2 h ramp up and followed by natural cooling (Seabold 2015).

Literature reports on phase transitions:

1) Shannon 1972 performed differential thermal analysis (DTA) on the starting material α-$Cu_3V_2O_8$ and found two endotherms upon heating at 500°C and 725°C. The phase transition occurred at 500°C and was followed by decomposition at 725°C. The paper did not illustrate what this new phase is.
2) Rao 1993 observed a reversible phase transition in $Cu_3V_2O_8$ by DTA analysis and in-situ high temperature XRD. The paper notes two high temperature polymorphs of $Cu_3V_2O_8$, β- and γ-$Cu_3V_2O_8$, in addition to the room temperature phase α- $Cu_3V_2O_8$. The two transition temperatures from α to β and from β to γ are at 510 and 545°C, respectively. The α-phase seems to match the phase found in Brisi 1958. The ICSD card also comments that the α-phase can be the same phase of the single crystal phase in Coing-Boyat 1982. The crystal structures of the so-called β and γ phases are not well documented.
3) Rogado 2003 confirmed a phase transition from α to β, triclinic to monoclinic.
4) Min 2011 confirmed a phase transition from β to γ, monoclinic to triclinic. The $Cu_3V_2O_8$ precursor $Cu_3V_2O_7(OH)_2{\cdot}2H_2O$ was calcined at different temperatures for 4 h. At 500°C, the phase was monoclinic β-$Cu_3V_2O_8$; when the temperature rose to 700°C, the phase was triclinic γ-$Cu_3V_2O_8$. We refer to this high temperature phase as γ; the original paper did not use this terminology.

2. Temperature profile for annealing PVD libraries

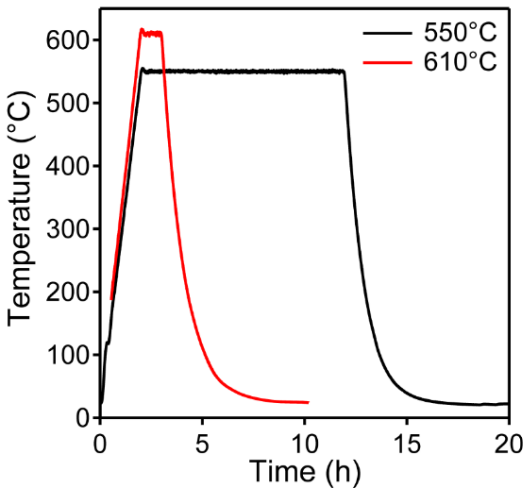

Figure S1. Temperature profiles of the annealing process in the Thermo Scientific box oven with flowing air. Library A (black line) was heated at 550°C for 10 hours and Library B (red line) was heated at 610°C for 1 hour. The annealing was preceded by a 2 h temperature ramp and followed by natural cooling.

3. Phase fractions from XRD analysis

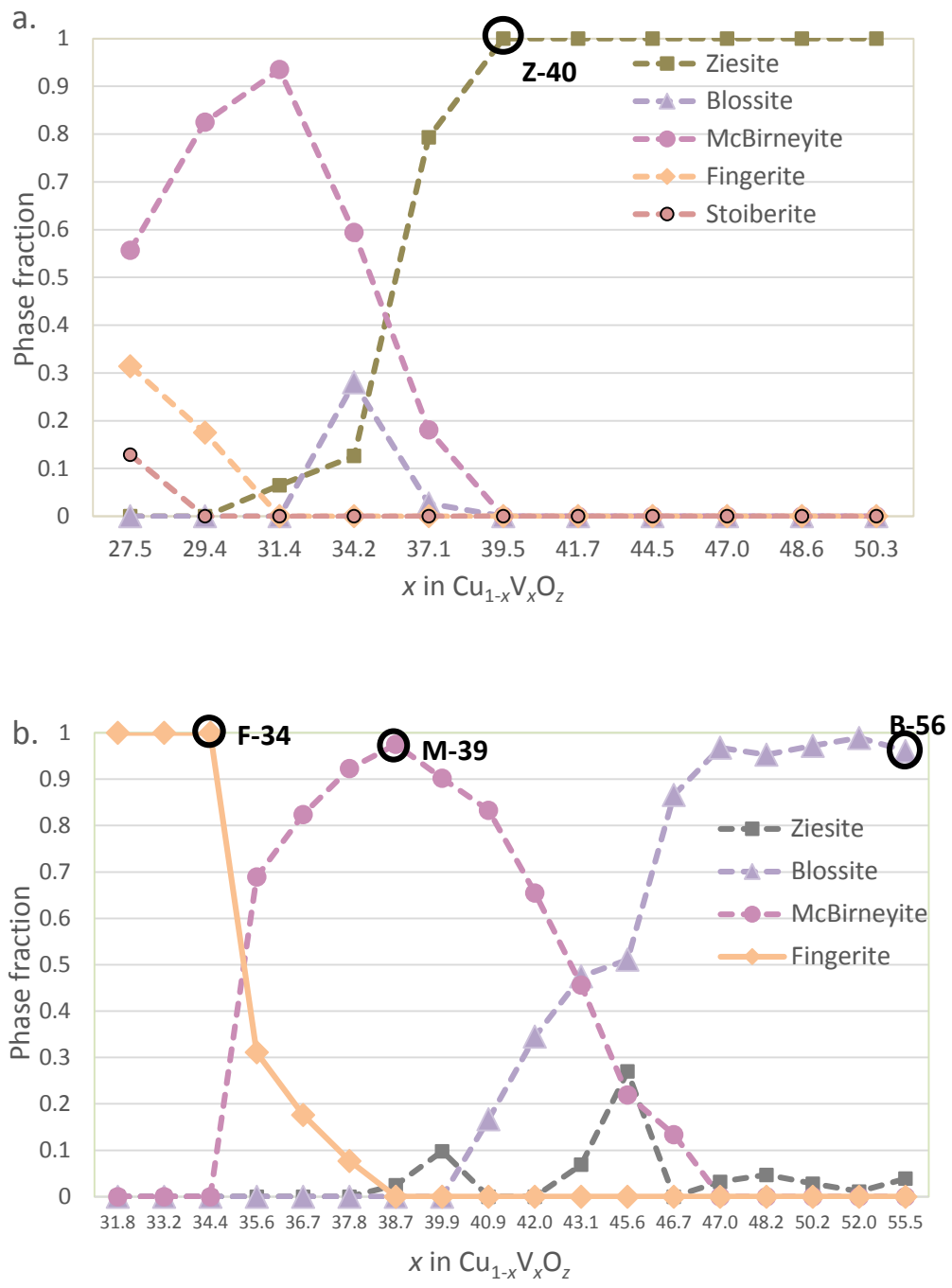

Figure S2. X-ray diffraction phase fraction data plotted against Vanadium content for (a.) library A and (b.) library B. The 4 samples used for optical characterization are circled and labelled.

Phase fraction data from XRD analysis are shown in Figure S2 and included in the manuscript in Figure 3. Phase fraction is estimated from X-ray diffraction measurements and plotted versus EDS measurements of x in $Cu_{1-x}V_xO_z$. XRD data was measured at 11 evenly spaced points in library A and 18 evenly spaced points in library B. Labels F-34, M-39, Z-40, and B-56 refer to specific samples where optical properties were characterized by ultraviolet-visible (UV-Vis) spectroscopy (see Figure 5 in the manuscript).

4. Chemical stability measurements

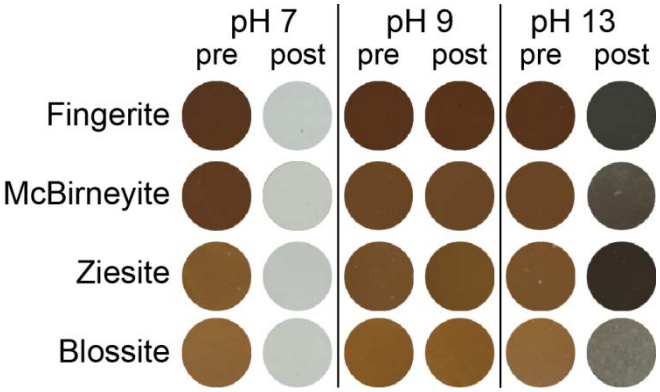

Figure S3. Images of 2mm-diameter thin film samples pre- and post-soaking in electrolyte solution for 48 hours.

To ascertain the chemical stability of the different phases, composition libraries were soaked in electrolyte solution for 48 hours. Samples exhibiting primarily Ziesite and Fingerite phases were chosen from a library annealed at 610 ^{o}C and samples exhibiting primarily Blossite and McBirneyite were chosen from a library annealed at 550 ^{o}C. Electrolyte solutions (pH 7, pH 9 and pH 13) were prepared as described in the manuscript and 1 L of solution was used for each soaking experiment so that given the total Cu and V content of the libraries, the molality could not exceed 50 µM. The samples were imaged in reflection mode using an EPSON Perfection V600 photoscanner and 2 mm-diameter images are shown both pre-soak (as-prepared) and post-soak (after 48 hours) for each phase. Each sample has a deep orange color as-prepared with Fingerite having the darkest appearance. After the 48 soak in pH 7 electrolyte, the samples appear to be completely dissolved, as the "post" images in Figure S3 are equivalent to the bare substrate. In pH 9 electrolyte, the samples appear to be unchanged. In pH 13 electrolyte, each sample is substantially darkened; further investigation is required to understand the chemical modifications to the samples.

5. Chopped-illumination CVs and data processing

Cyclic voltammetry (CV) was performed with a starting potential of 1.23 V vs RHE, scanning down to 0.79 V vs RHE, then back to the starting potential at a rate of 20 mV s^{-1}. After an initial dark interval of 0.5 seconds, the 385 nm LED illumination was toggled using 50% duty cycle over 1 second periods. Data was acquired in every 0.2 mV, yielding 50 data points for each light and each dark interval.

Photovoltage from CV data was calculated using a polynomial fitting algorithm written in R. The algorithm starts by identifying the CV sweep directions from the sign of dE_{we}/dt at each data point (where E_{we} is the

working electrode voltage) so that cathodic and anodic sweeps are considered separately (Figure S4). The data is then factored according to light and dark intervals. To mitigate the transient current spike observed at the time of LED switching, the first 35 data points and last 5 data points are omitted from each interval and the remaining points are averaged (Figure S5). Third order polynomial fits are applied to the light and dark interval averages, respectively (Figure S6). The dark fit is then subtracted from the light fit, yielding a representative anodic photocurrent as a function of potential for a given sample. A data frame is compiled by applying the fitting algorithm over the entire set of samples with varying composition (Figure S7).

Many samples exhibit anodic photocurrent even at the most cathodic potentials, and for many samples the small anodic photocurrent is not strongly dependent on potential for the most cathodic illumination cycles, creating large uncertainty for an extrapolation to zero photocurrent. Since the illuminated open circuit potential is not directly measured, we define a related parameter, the potential where photocurrent falls to a minimum critical value. The critical value was shown to be 85 µA cm^{-2} because each sample reached that low of a photocurrent during the CV.

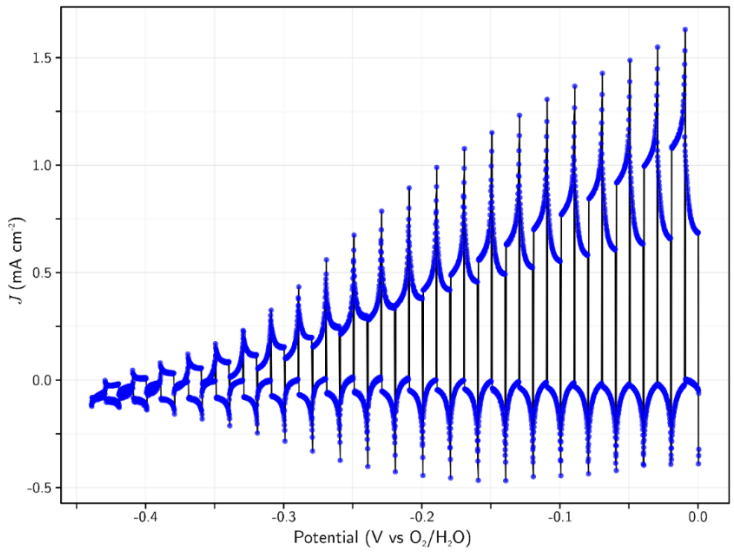

Figure S4. A plot of raw CV data, sweeping from the O_2/H_2O redox potential (1.23 V vs. RHE) to -0.44 V (0.79 V vs. RHE), and back at a rate of 20 mV s^{-1}.

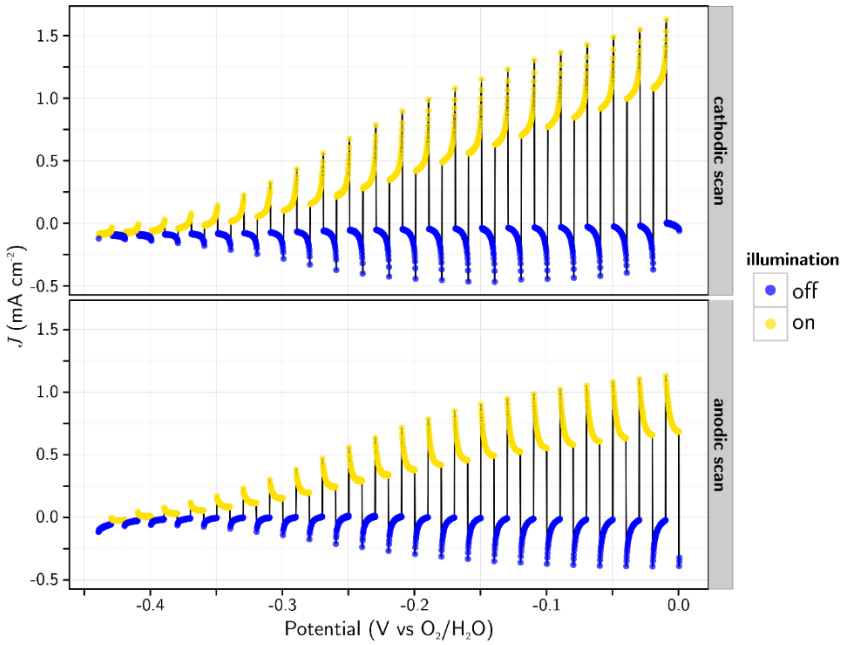

Figure S5. Data from Figure S4 separated into cathodic and anodic scan directions, then factored according to intervals of illumination on/off.

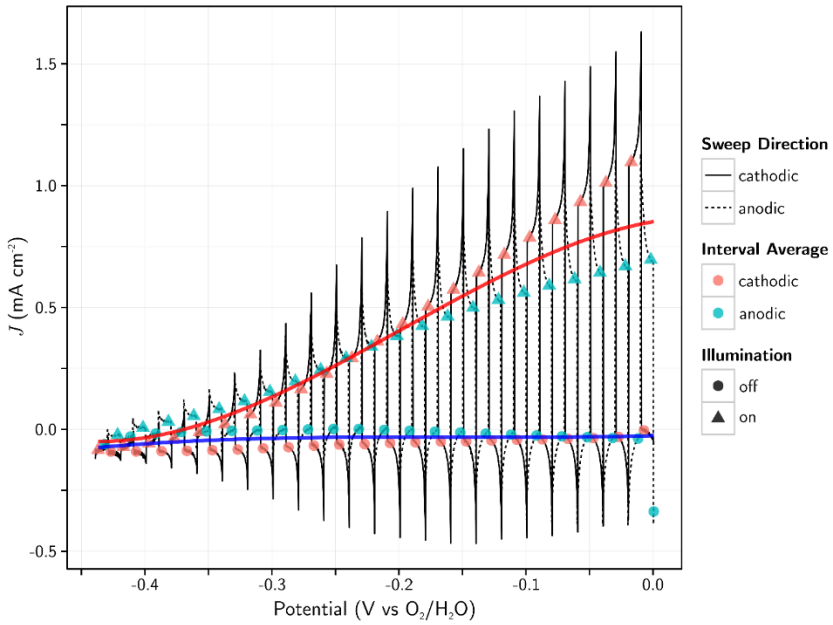

Figure S6. An example of polynomial fitting to the illumination on/off interval averages. The initial 70% of data points after light switching are omitted from the interval average to mitigate the inclusion of current transients in the measured photocurrent. The dark current fit (blue) is subtracted from the light current fit (red) to yield the representative photocurrent function.

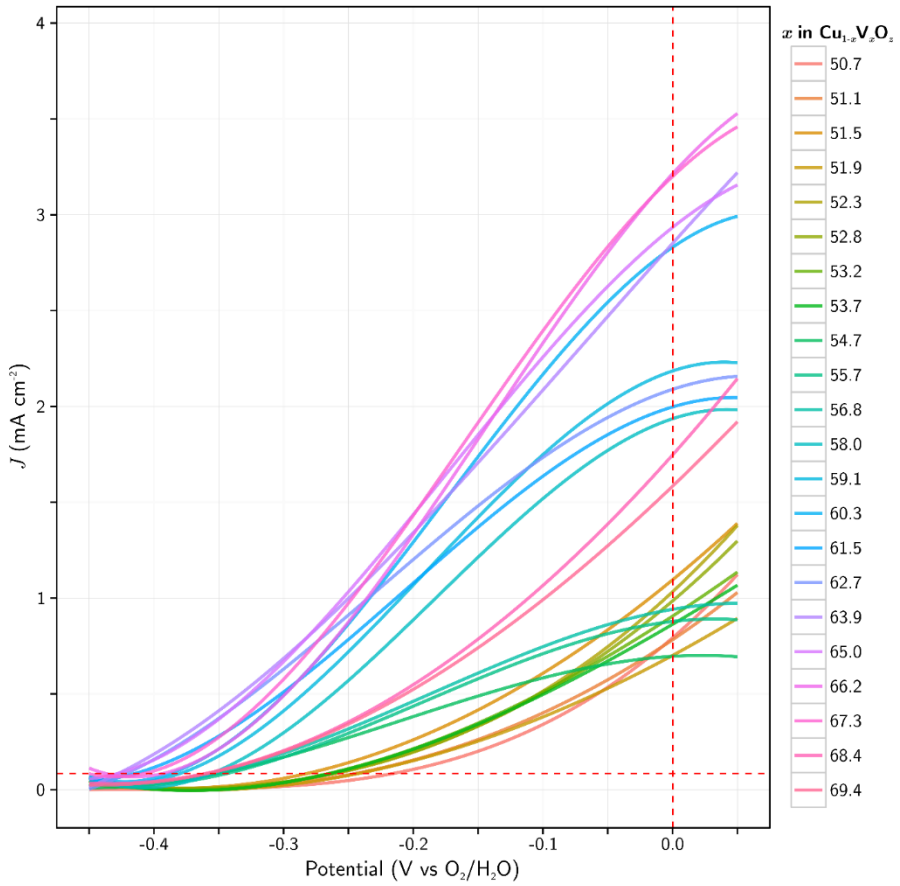

Figure S7. A plot of the representative photocurrent functions for all measured compositions in library A after polynomial fitting from Figure S6. Short circuit current density (J_{sc}) is taken from the y-intercept with the dashed red vertical line. Photovoltage (V_{μ}) at J = 0.085 mA cm^{-2} is taken from the x-intercept with the dashed red horizontal line.

References:

[1] J. M. Hughes, B. S. Christian, L. W. Finger, L. L. Malinconico, *J. Volcanol. Geotherm. Res.* **1987**, 33, 183.

[2] M. E. Zelenski, N. V. Zubkova, I. V. Pekov, M. M. Boldyreva, D. Yu. Pushcharovsky, A. N. Nekrasov, *European Journal of Mineralogy* **2011**, 23, 475.

[3] R. D. Shannon, C. Calvo, *Can. J. Chem.* **1972**, 50, 3944.

[4] N. Rogado, M. K. Haas, G. Lawes, D. A. Huse, A. P. Ramirez, R. J. Cava, *Journal of Physics: Condensed Matter* **2003**, 15, 907.

[5] W. Min, Q. Liu, *Adv. Mater. Res.* **2011**, 236-238, 1675.

[6] S. Zhang, Y. Sun, C. Li, L. Ci, *Solid State Sci.* **2013**, 25, 15.

[7] J. A. Seabold, N. R. Neale, *Chem Mater* **2015**, 150112115329007.

[8] C. Brisi, A. Molinari, *Annali di Chimica* **1958**, 48, 263.

[9] P. J. Coing-Boyat, *Acta Cryst.* **1982**, B38, 1546.

[10] N. S. Rao, O. G. Palanna, *Bull. Mater. Sci.* **1993**, 16, 261.